Binding of Ricin A-Chain to Negatively Charged Phospholipid Vesicles Leads to Protein Structural Changes and Destabilizes the Lipid Bilayer†

Philip J. Day, Teresa J. T. Pinheiro, Lynne M. Roberts, and J. Michael Lord*

Department of Biological Sciences, University of Warwick, Coventry CV4 7AL, U.K.

Received November 1, 2001; Revised Manuscript Received December 5, 2001

ABSTRACT: Ricin is a heterodimeric protein toxin in which a catalytic polypeptide (the A-chain or RTA) is linked by a disulfide bond to a cell-binding polypeptide (the B-chain or RTB). During cell entry, ricin undergoes retrograde vesicular transport to reach the endoplasmic reticulum (ER) lumen, from where RTA translocates into the cytosol, probably by masquerading as a substrate for the ER-associated protein degradation (ERAD) pathway. In partitioning studies in Triton X-114 solution, RTA is predominantly found in the detergent phase, whereas ricin holotoxin, native RTB, and several single-chain ribosome-inactivating proteins (RIPs) are in the aqueous phase. Fluorescence spectroscopy and far-UV circular dichroism (CD) demonstrated significant structural changes in RTA as a result of its interaction with liposomes containing negatively charged phospholipid (POPG). These lipid-induced structural changes markedly increased the trypsin sensitivity of RTA and, on the basis of the protein fluorescence determinations, abolished its ability to bind to adenine, the product resulting from RTA-catalyzed depurination of 28S ribosomal RNA. RTA also released trapped calcein from POPG vesicles, indicating that it destabilized the lipid bilayer. We speculate that membrane-induced partial unfolding of RTA during cell entry may facilitate its recognition as an ERAD substrate.

Ricin is a potent cytotoxin from the seeds of *Ricinus communis* that is composed of an RNA *N*-glycosidase A-chain (RTA)[1] disulfide-bonded to a cell-binding B-chain (RTB). RTB, a galactose-specific lectin, binds to cell surface receptors, thereby facilitating entry of the toxin into cells by receptor-mediated endocytosis (*1*). Once inside the cell, ricin is transported, in a retrograde direction, to the endoplasmic reticulum (ER). It is understood that the lectin function of RTB is crucial for this transport, possibly through binding to galactosylated proteins that recycle between the Golgi apparatus and the ER (*2*). By analogy with cholera toxin (*3*) and mistletoe lectin (*4*), it is likely that on reaching the ER the disulfide bond connecting RTA and RTB is reductively cleaved and that free RTA is targeted to the Sec61 complex for retrotranslocation into the cytosol. Having reached the cytosol, the reduced RTA catalytically inactivates ribosomes by depurination of a specific adenyl residue (A_{4324} in the rat sequence) of 28S ribosomal RNA, rendering the ribosome incapable of binding elongation factors and hence inhibiting protein synthesis (*5*). This, in turn, results in cell death.

It is now recognized that RTA is a member of a large family of plant-derived ribosome-inactivating proteins (RIPs) that share a similar structure and can be divided into two classes. Type I RIPs are composed solely of a single polypeptide chain with RTA-like *N*-glycosidase activity, and they cannot therefore efficiently enter cells. Type II RIPs are composed of a type I RIP covalently linked to a cell-binding B-chain. They are therefore potently cytotoxic.

Retrograde transport of ricin and a number of other toxins, such as cholera toxin, Shiga toxin, Shiga-like toxin (SLT), and *Pseudomonas* exotoxin (PE), from the cell surface to the ER is now well established (*6*−*9*). The A-chains of such toxins are thought to translocate from the ER into the cytosol via the Sec61 translocon (*7, 8*). For toxins, passage to these channels may be rendered possible by exploiting the ER-associated protein degradation (ERAD) pathway, a quality-control process of the ER. ERAD normally deals with newly synthesized ER-targeted proteins that fail to fold correctly or which are unassembled components of an oligomeric complex (*10*−*12*). Such proteins are recognized by luminal ER chaperones, delivered to the Sec61 complex, and then retrotranslocated into the cytosol. If appropriate, such proteins are deglycosylated before being polyubiquitinated and degraded by the proteasome (*11, 12*). It would appear that a proportion of the translocated toxins avoid the degradative fate of this process, due in part to the presence of an abnormally low number of lysyl residues in their A-chains (*13, 14*). This reduces the chance of ubiquitination and thereby prevents efficient targeting to the proteasome. Despite increasing evidence for the involvement of the ERAD pathway in the intoxication process, the features of toxins that permit their recognition as ERAD substrates remain unclear.

† Supported by a Wellcome Trust Program Grant to L.M.R. and J.M.L.

* To whom correspondence should be addressed. Phone: (44) 2476 523598. Fax: (44) 2476 523701. E-mail: mlord@bio.warwick.ac.uk.

[1] Abbreviations: RTA, ricin A-chain; RTB, ricin B-chain; ER, endoplasmic reticulum; ERAD, ER-associated protein degradation; SLT, Shiga-like toxin; RIP, ribosome-inactivating protein; CD, circular dichroism; POPG, 1-hexadecanoyl-2-[*cis*-9-octadecanoyl]-*sn*-glycero-3-[phospho-*rac*-(1-glycerol)]; DOPC, 1,2-di[*cis*-9-octadecanoyl]-*sn*-glycero-3-phosphocholine; DMPC, 1,2-ditetradecanoyl-*sn*-glycero-3-phosphocholine; DPPC, 1,2-dihexadecanoyl-*rac*-glycero-3-phosphocholine; DMPA, 1,2-ditetradecanoyl-*sn*-glycero-3-phosphate.

10.1021/bi012012i CCC: $22.00
Published on Web 01/29/2002

A common feature of A-chains of ER-directed toxins is the presence of a hydrophobic patch of amino acids that becomes solvent-exposed upon separation of the A- and B-chains (*15*, *16*). It is therefore possible that this exposed hydrophobic surface is recognized by ER chaperones to assist in targeting to the Sec61 complex. Alternatively, exposure of this hydrophobic region in the ER lumen could facilitate interaction of the A-chain with the ER membrane, either allowing direct access to the Sec61 translocons or causing partial unfolding of the A-chain, allowing recognition by the ERAD machinery. It has been demonstrated that the hydrophobic patch of RTA (residues 238−267) can act as a signal peptide if fused to the N-terminus of a target protein (*17*). Similarly, a peptide derived from the hydrophobic patch from Shiga-like toxin (SLT) has been shown to insert into membranes (*16*). Furthermore, introduction of charged residues into the hydrophobic patch of SLT greatly reduced cytotoxicity without affecting catalytic activity (*16*), and site-directed mutagenesis has also suggested a role for the C-terminal hydrophobic region of ricin in cytotoxicity (*18*).

A number of reports have suggested that ricin or subunits thereof can interact with a variety of model membrane systems, but no clear picture has emerged (*19*−*24*). For example, it has been shown that RTA can fuse DPPC and DMPC vesicles and cause alterations in the phase transition temperature for DPPC vesicles (*19*), that ricin holotoxin changes the T_m of DPPC vesicles (*20*), that both RTA and RTB can bind to and insert into PC vesicles (*21*), and that ricin holotoxin can cause vesicle fusion (*22*, *23*). Furthermore, it has been suggested that RTB may possess phospholipase activity and that this activity could be responsible for membrane translocation of ricin (*24*, *25*).

RTA has a single tryptophan residue (Trp 211) and 14 tyrosyl residues (at positions 6, 21, 80, 84, 91, 115, 123, 152, 153, 154, 183, 194, 243, and 257). Trp 211, Tyr 80, and Tyr 123 are highly conserved among plant RIPs and form part of the active site. We have used both tryptophan and tyrosine fluorescence, along with far-UV CD, to investigate changes in RTA structure on interaction with phospholipid vesicles. In this study, we demonstrate that ricin A-chain, but not ricin holotoxin, interacts with negatively charged phospholipid vesicles. Interaction of RTA with such vesicles results in both secondary and tertiary structural changes that dramatically increase sensitivity to protease digestion. Conceivably, RTA released from ricin in the ER during cell entry could interact with the luminal surface of the ER membrane. If this interaction also triggers structural changes in the protein, it may permit recognition of RTA as a misfolded protein by the ERAD machinery and thereby facilitate translocation into the cytosol.

MATERIALS AND METHODS

Materials. 1-Hexadecanoyl-2-[*cis*-9-octadecanoyl]-*sn*-glycero-3-[phospho-*rac*-(1-glycerol)] (POPG), 1,2-di[*cis*-9-octadecanoyl]-*sn*-glycero-3-phosphocholine (DOPC), 1,2-ditetradecanoyl-*sn*-glycero-3-phosphocholine (DMPC), 1,2-dihexadecanoyl-*rac*-glycero-3-phosphocholine (DPPC), 1,2-ditetradecanoyl-*sn*-glycero-3-phosphate (DMPA), trypsin (TPCK treated), Triton X-114, momordin, saporin, gelonin, trichosanthin, and ricin were all from Sigma. Calcein was from Molecular Probes. Pokeweed antiviral protein was a gift from Dr Martin Hartley.

Expression and Purification of Ricin A-Chain. A 50 mL culture of plasmid-bearing *Escherichia coli* JM101 was grown overnight at 37 °C. This starter culture was used to inoculate 500 mL of 2YT media and the culture grown for 2 h at 30 °C. RTA expression was induced by addition of 0.1 mM isopropyl 1-thio-β-D-galactoside (IPTG) for 4 h at 30 °C. Cells were harvested by centrifugation at 5000 rpm, resuspended in 15 mL of 5 mM sodium phosphate buffer, pH 6.3, and broken by sonication. Cell debris was removed by centrifugation at 15 000 rpm for 60 min at 4 °C and the RTA-containing supernatant loaded onto a carboxymethyl-Sepharose CL-6B column (Pharmacia) equilibrated in the same buffer. The column was washed with 1000 mL of buffer, followed by 100 mL of buffer containing 100 mM sodium chloride to remove unbound proteins. RTA was eluted with a 500 mL NaCl gradient (100−300 mM). Fractions containing pure RTA were identified by SDS−PAGE, pooled, and stored at 4 °C.

Preparation of Triton X-114. Triton X-114 (2 mL) was added to 98 mL of 10 mM Tris-HCl, pH 7.6, 150 mM KCl containing 1.6 mg of butylated hydroxytoluene and dissolved by stirring on ice for 1 h. After warming to 30 °C, the phases were allowed to separate, and the upper aqueous phase was discarded. The Triton X-114 phase was washed a further 3 times with 10 mM Tris-HCl, pH 7.6, 150 mM KCl, and the concentration of the final stock was determined from the absorbance at 275 nm (*25*). For partitioning experiments (*26*), ricin (2 μg/mL), RTB (1 μg/mL), or RTA (1 μg/mL) was incubated at 30 °C for 30 min in 20 mM sodium phosphate, pH 7.1. The samples were cooled on ice; Triton X-114 was added to 1% (v/v) and incubated for a further 30 min. Following incubation at 30 °C for 3 min, the aqueous and detergent phases were separated by centrifugation, and protein was precipitated with 50% (v/v) acetone at room temperature.

Preparation of Lipid Vesicles. Lipids were dissolved in chloroform, and a lipid film was prepared by drying under vacuum overnight. DMPA lipid films were prepared by dissolving the lipid in chloroform/methanol (3:1) with the addition of a few drops of ammonia solution. Lipid films were hydrated in 20 mM sodium phosphate, pH 7.1, and freeze−thawed 6 times. Small unilamellar vesicles were formed by extruding the lipid through a 100 μm filter 6−7 times. Vesicles were stored at 4 °C. To incorporate calcein into vesicles, 20 mM sodium phosphate, pH 7.1, containing 10 mM calcein was used to resuspend the lipid films and the preparation of vesicles continued as above. Nonincorporated calcein was removed by passage through a PD10 size exclusion column.

Interaction of RIPs with Lipid Vesicles. Vesicles were diluted to give an appropriate concentration in 200 μL of sodium phosphate buffer, pH 7.1. To this was added an equal volume of RIP in the same buffer. Binding was allowed to proceed for 1 h prior to detection of bound species by CD, fluorescence, or ultracentrifugation. Centrifugation was used to separate bound from unbound RIP as follows. The 400 μL binding reaction was carefully layered onto a 3 mL pad of 0.25 M sucrose in 20 mM sodium phosphate, pH 7.1. Vesicles were pelleted by centrifugation in a Beckman TL-100 ultracentrifuge at 100 000 rpm for 1 h. Fractions (0.5 mL) were removed from the top, and the pellet was

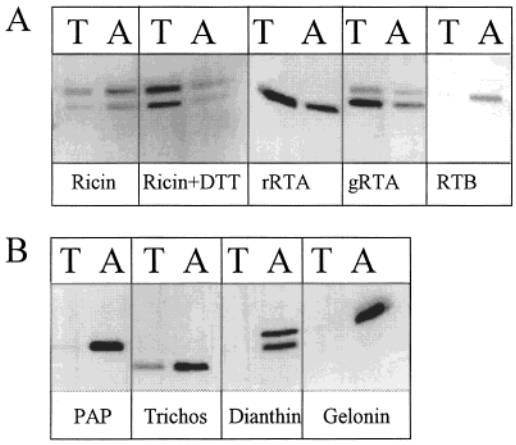

FIGURE 1: Partitioning of RIPs into Triton X-114. (A) Ricin (2 μg/mL) was incubated at 30 °C for 30 min in the presence or absence of 10 mM DTT. Recombinant (r)RTA, native (g)RTA, and RTB (1 μg/mL) were incubated as above in the absence of DTT. The samples were cooled on ice, and Triton X-114 was added to 1% (v/v) and incubated for a further 30 min. Following a brief incubation at 30 °C (3 min), the aqueous phase (A) and detergent phase (T) were separated by centrifugation, and the protein was precipitated with acetone. (B) PAP, trichosanthin (Trichos), dianthin, and gelonin (1 μg/mL) were incubated at 30 °C for 30 min in the absence of DTT. The detergent phase (T) and aqueous phase (A) were mixed with acetone, and precipitated protein was separated by SDS−PAGE.

resuspended in 0.5 mL of 0.1% (w/v) SDS. Fractions were analyzed by SDS−PAGE.

Fluorescence Spectroscopy. Fluorescence spectra were recorded on a Photon Technology International fluorometer at 20 °C with 1 nm slit widths, 0.5 s integration times, and 1 nm step size using a 4 mm path length cuvette. Typically 4 spectra were averaged. Protein concentrations were in the range 0.4−5 μM in 20 mM sodium phosphate, pH 7.1. All spectra had appropriate buffer blanks subtracted.

Circular Dichroism. Far-UV CD was measured on a Jasco J-715 spectrapolarimeter at 20 °C using a 1 mm path length cuvette. Typically 8 spectra were recorded from 190 to 260 nm with 1 nm step size and averaged. Spectra were corrected for background by subtraction of appropriate blanks.

RESULTS

Partitioning of RTA into Detergent. At neutral pH, ricin holotoxin largely remains in the aqueous phase following incubation with Triton X-114 and subsequent phase separation (Figure 1A). In contrast, recombinant RTA and plant-derived RTA both substantially partition into the detergent phase under the same conditions (Figure 1A). Purified RTB, like ricin, remains in the aqueous phase (Figure 1A); however, following incubation of ricin with Triton X-114 in the presence of 10 mM DTT, both of the separated chains partition into the detergent phase (Figure 1A). This difference in the ability of RTB to partition into detergent is probably a function of the integrity of the four internal disulfide bonds, such that reduction in the presence of detergent allows reduction of the internal disulfide bonds, resulting in unfolding and detergent solubility. In marked contrast to RTA, structurally related type I RIPs (pokeweed antiviral protein, PAP; trichosanthin; dianthin; gelonin), that lack a C-terminal hydrophobic region, did not partition into detergent (Figure 1B).

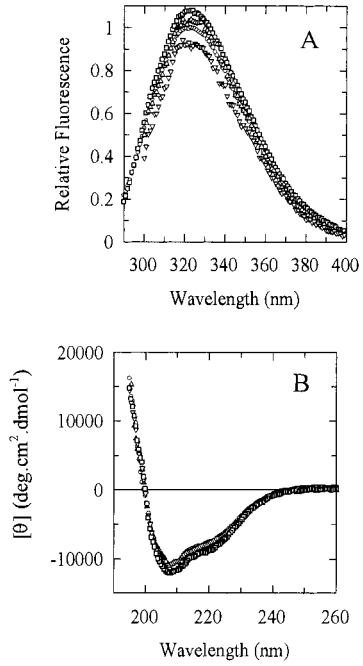

FIGURE 2: (A) Fluorescence emission spectra of RTA (5 μM) in the absence (○) or presence of 2.5 mM DOPC (□), 2.5 mM DMPC (△), and 2 mM DPPC (▽) in 20 mM phosphate buffer, pH 7.1, at 20 °C. Spectra were normalized against the fluorescence intensity at λ_{max} for RTA in the absence of lipid. Excitation wavelength was 280 nm. (B) Far-UV CD spectra of RTA in the absence (○) or presence of 2 mM DOPC (□), 2 mM DMPC (△), and 2 mM DPPC (▽) in 20 mM phosphate buffer, pH 7.1, at 20 °C.

Interaction of Ricin and RTA with Phosphatidylcholine (PC) Vesicles. Previous reports have suggested that ricin and RTA can alter the properties of a variety of PC vesicles (*19*−*23*). In the present study, we have used fluorescence spectroscopy and circular dichroism (CD) to investigate changes in the structure of the protein on interaction with lipid vesicles. The fluorescence emission spectrum of RTA, following excitation at 280 nm (Figure 2A), shows that RTA has a λ_{max} of ∼321 nm. Incubation of RTA with various phosphatidylcholine vesicles did not alter the intrinsic protein fluorescence spectrum (Figure 2A), suggesting that if RTA bound to these vesicles then the interaction did not result in significant changes in the structure of the protein. Similarly, the far-UV CD spectrum of RTA was also unchanged in the presence of phosphatidylcholine vesicles, suggesting that there are no significant secondary structural changes (Figure 2B). Incubation of ricin holotoxin with DOPC vesicles also had no effect on the intrinsic fluorescence of the protein (data not shown).

Interaction of RTA with Negatively Charged Phospholipid Vesicles. RTA was incubated with different concentrations of POPG and the effect on intrinsic protein fluorescence monitored following excitation at 280 nm. Incubation of RTA with relatively low concentrations of POPG caused a large blue shift in the intrinsic protein fluorescence spectrum (Figure 3A). The wavelength of maximum fluorescence (λ_{max}) was blue shifted by 17 nm, from 321 nm in free solution to 304 nm in the presence of POPG. Titration with very low concentrations (up to ∼10 μM) of POPG quenched the intrinsic fluorescence of RTA whereas further increasing the concentration of POPG caused a progressive blue shift in λ_{max} and recovery of fluorescence intensity. The maximum

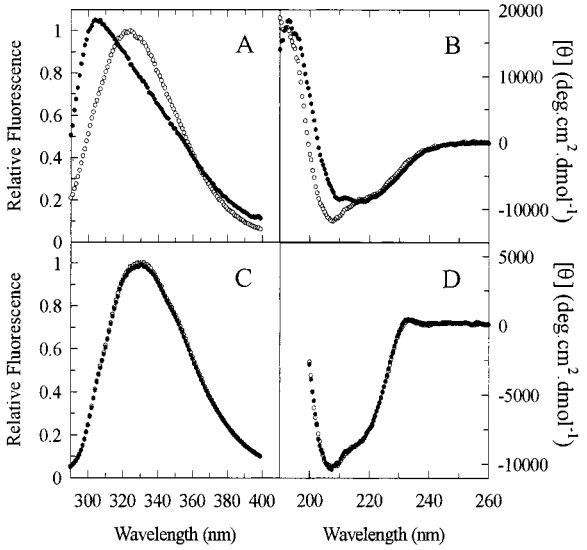

FIGURE 3: Fluorescence emission spectra of RTA (A) and ricin (C) in the absence (○) or presence (●) of 200 μM POPG in 20 mM phosphate buffer, pH 7.1, at 20 °C. Spectra were normalized against the fluorescence intensity at λ_{max} for RTA in the absence of lipid. Excitation wavelength was 280 nm. Far-UV CD spectra of RTA (B) and ricin (D) in the absence (○) or presence (●) of 200 μM POPG in 20 mM phosphate buffer, pH 7.1, at 20 °C.

change in λ_{max} occurred at ~200 μM POPG, and higher concentrations had only minor effects on the fluorescence spectrum.

Incubation with POPG vesicles also had a significant effect on the far-UV CD spectrum of RTA (Figure 3B). As seen for the changes in intrinsic fluorescence, only low concentrations of POPG were required to cause substantial changes in the spectrum. Increasing concentrations of POPG resulted in a steady decrease in the minima at 208 nm. Analysis of the far-UV CD spectra predicted 35% helical content and 18% β-sheet for RTA in solution, in good agreement with the known crystal structure. On binding to POPG vesicles, the predicted helical content decreased by ~3% while the proportion of β-sheet increased by ~4%.

Ricin holotoxin did not display any significant difference in intrinsic fluorescence (Figure 3C) or far-UV CD (Figure 3D) following incubation with POPG vesicles, suggesting that the presence of RTB in the holotoxin prevents binding of the RTA moiety to the POPG vesicles. This is consistent with the observation that ricin holotoxin must be reduced before RTA can partition into Triton X-114.

Previous reports have suggested that the single tryptophan residue (Trp 211) of RTA penetrates the lipid bilayer on interaction of RTA with vesicles (*27*). To investigate if the large change in the fluorescence emission spectrum of RTA on binding to POPG was only due to changes in the environment of Trp 211, the fluorescence experiments were repeated with an excitation wavelength of 295 nm, to excite tryptophan alone. Increasing concentrations of POPG resulted in a fluorescence quench following excitation at 295 nm such that at 200 μM POPG the fluorescence intensity at 326 nm (λ_{max}) was reduced by ~60% (Figure 4A). Changes in λ_{max} following excitation at 295 nm were rather different from that observed with excitation at 280 nm. In marked contrast to the 17 nm blue shift observed on excitation at 280 nm, excitation at 295 nm caused an 8 nm red shift in λ_{max}, suggesting that the changes in fluorescence observed previously were due predominantly to tyrosyl residues. To investigate this further, excitation wavelengths of 260 and 270 nm were employed. In both cases, a ~17 nm blue shift was observed in the presence of 200 μM POPG (data not shown).

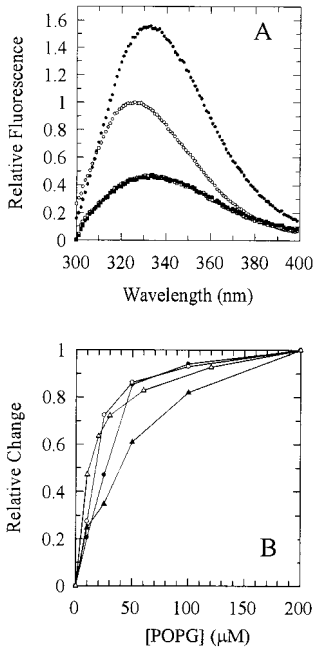

FIGURE 4: (A) Fluorescence emission spectra of RTA in the absence (circles) or presence (squares) of 200 μM POPG in 20 mM phosphate buffer, pH 7.1, at 20 °C following excitation at 295 nm either with (solid symbols) or without (open symbols) the addition of 10 mM adenine. Spectra were normalized against the fluorescence intensity at λ_{max} for RTA in the absence of lipid and corrected for the inner filter in the presence of adenine. (B) Effect of increasing POPG concentration on RTA fluorescence intensity at 300 nm (○) and λ_{max} (●) following excitation at 280 nm, fluorescence intensity at 320 nm (△) following excitation at 295 nm and far-UV CD at 208 nm (▲).

The product of the RTA-catalyzed depurination of 28S rRNA is adenine, and binding of adenine to RTA results in a large enhancement in tryptophan fluorescence (*27*). To determine if the structural changes observed in RTA on interaction with POPG vesicles affected the structure and function of the active site, the ability of RTA to bind adenine in the presence of vesicles was tested. Addition of 10 mM adenine to RTA in buffer alone resulted in a ~160% increase in tryptophan fluorescence, consistent with earlier observations [Figure 4A and (*27*)]. However, no such increase in intrinsic fluorescence was observed on addition of adenine to POPG-bound RTA (Figure 4A).

Plotting the changes in far-UV CD at 208 nm, fluorescence intensity at 300 nm, and fluorescence λ_{max} (λ_{ex} 280 nm) and fluorescence intensity at 320 nm (λ_{ex} 295 nm) against concentration of POPG (Figure 4B) showed that the changes in RTA far-UV CD and fluorescence occur over roughly the same POPG concentration range (with half-maximal changes at ~37, ~20, ~25, and ~15 μM, respectively).

To investigate whether the accessibility of the tryptophan residue or tyrosyl residues changed on binding to POPG, iodide quenching experiments were performed (data not shown). With excitation at 280 nm, Stern−Volmer quenching coefficients of 0.70 and 0.63 M^{-1} were observed for RTA in the absence and presence of POPG vesicles, respectively.

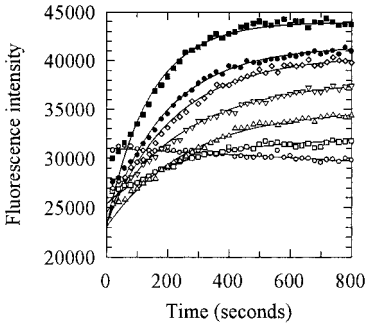

FIGURE 5: Time-dependent change in the intrinsic protein fluorescence of RTA on incubation with POPG. RTA (2.5 μM) was incubated in the absence (○) or presence of 10 (●), 20 (□), 30 (■), 60 (△), 120 (▲), and 200 μM (▽) POPG at 20 °C. Emission at 300 nm was monitored continuously with excitation at 280 nm.

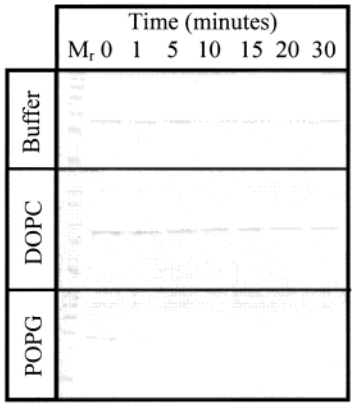

FIGURE 6: Effect of incubation of RTA with lipid vesicles on its sensitivity to trypsin. RTA (0.1 mg/mL) was incubated for 1 h in 20 mM phosphate buffer, pH 7.1, in the absence or presence of 200 μM lipid prior to addition of 1% (w/w) trypsin and digestion at 37 °C. Aliquots were removed at timed intervals and boiled in SDS−PAGE loading buffer.

At 295 nm the corresponding Stern−Volmer coefficients were 0.88 and 0.87 M^{-1}. Thus, it was concluded that the accessibility of the chromophores did not change significantly on interaction with POPG.

The change in intrinsic RTA fluorescence on interaction with POPG is a time-dependent process. Figure 5 shows time courses for the changes in fluorescence emission at 300 nm (λ_{ex} 280 nm) that occur on addition of different concentrations of POPG to a fixed concentration of RTA. The data can be fitted to single exponential curves with amplitudes dependent on the concentration of added POPG. In contrast, the calculated rates remained relatively constant with a mean of 0.28 ± 0.08 min^{-1}. All of the curves extrapolated to the same initial starting fluorescence intensity; however, this did not correlate with the observed fluorescence in the absence of lipid, suggesting that in these manual mixing experiments a fast initial fluorescence quenching step has been missed. Indeed, although the curves fitted the overall data well, the initial data points fitted rather poorly to the exponential curves, again suggesting an additional step that is not well resolved.

POPG-Bound RTA Is Protease-Sensitive. RTA free in solution is relatively resistant to proteolysis by trypsin (*28*) with virtually no digestion observed in the presence of 1% (w/w) trypsin for 1 h at 37 °C (Figure 6). Addition of DOPC vesicles (200 μM) had no effect on the resistance of RTA to tryptic digestion, in keeping with the observation that RTA

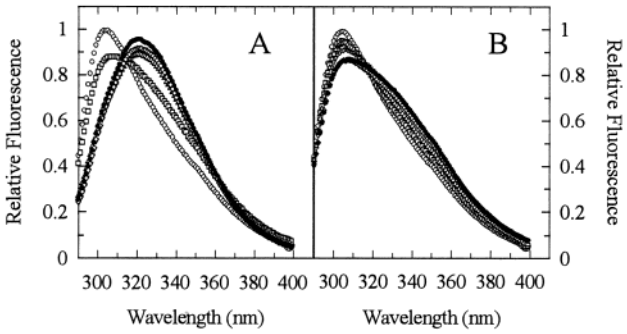

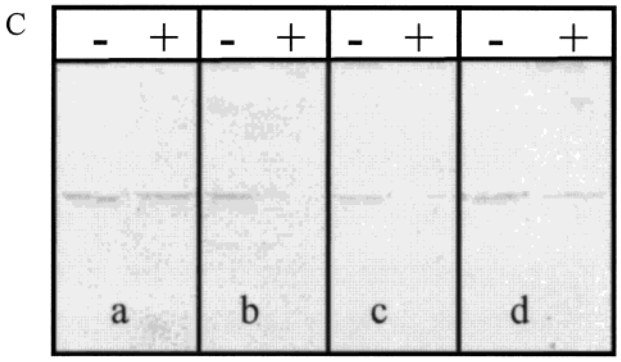

FIGURE 7: Effect of NaCl concentration on the binding of RTA to POPG vesicles. (A) POPG vesicles (200 μM) were incubated for 1 h at 20 °C in 20 mM phosphate buffer, pH 7.1 (○), containing 50 (□), 100 (△), 200 (▽), 300 (◇), or 500 mM NaCl (●) prior to addition of RTA (5 μM) and incubation for a further hour. (B) POPG vesicles (200 μM) were incubated with RTA (5 μM) for 1 h at 20 °C in 20 mM phosphate buffer, pH 7.1, prior to addition of NaCl (as above) and incubation for a further hour. (C) Following incubation of RTA (0.1 mg/mL) for 1 h in the absence (a) or presence (b) of POPG vesicles, trypsin [1% (w/w)] was added and digestion allowed to proceed for 15 min. (c) RTA was bound to POPG vesicles as in (b). After 1 h, NaCl was added to 100 mM, and after a further hour, trypsin was added and digestion was allowed to proceed for 15 min. (d) RTA was added to POPG vesicles that had been preincubated with 100 mM NaCl. After 1 h, tryptic digestion was carried out as above. Trypsin digestion was terminated by addition of SDS loading buffer and heating to 95 °C. Trypsin-treated (+) and -untreated samples (−) were analyzed by SDS−PAGE.

did not appear to interact with these vesicles. In contrast, RTA became exquisitely sensitive to trypsin in the presence of POPG vesicles (200 μM), with almost total digestion occurring within 5−10 min. Thus, changes in secondary and tertiary structure upon incubation with POPG vesicles can therefore be correlated with increased protease sensitivity.

To probe the nature of the interaction between RTA and POPG vesicles, the effect of ionic strength on vesicle binding was investigated. Preincubation of the POPG vesicles with increasing concentrations of sodium chloride prior to addition of RTA totally blocked binding, suggesting that the initial binding step is predominantly driven by ionic interactions (Figure 7A). RTA challenged in this way remained resistant to trypsin treatment, confirming that the structure remained essential native. If RTA/POPG complexes were preformed and then challenged with sodium chloride, RTA remained bound to the vesicles (Figure 7B) and trypsin-sensitive (Figure 7C), suggesting that after binding to the surface of the vesicles, to some extent RTA inserts into the lipid bilayer.

Type I RIPs Do Not Bind to POPG Vesicles. As noted above, type I RIPs do not partition into the detergent layer

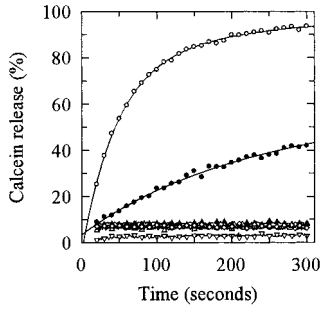

FIGURE 8: RIP-dependent release of calcein from calcein-loaded POPG vesicles. POPG vesicles (60 μM) containing 10 mM calcein were incubated at 20 °C with 1.5 μM momordin (▲), trichosanthin (△), saporin (▽), and ricin (◇), and with 0.4 (●) and 4 μM (○) RTA, and the increase in fluorescence at 512 nm was monitored continuously. 100% calcein release was calculated from the fluorescence intensity following addition of SDS. For clarity, only every 20th data point is illustrated.

following incubation with Triton X-114. We were therefore interested to see whether these RIPs could interact with POPG vesicles. Incubation of trichosanthin, momordin, dianthin, and saporin with 500 μM POPG vesicles had no effect on the fluorescence spectra of any of the proteins, suggesting that they did not interact significantly with these vesicles (data not shown).

RTA Releases Calcein from within POPG Vesicles. Incubation of RTA with calcein-loaded POPG vesicles resulted in a time-dependent release of calcein into the solution (Figure 8), but RTA was unable to release calcein from similarly loaded POPC vesicles (data not shown). The rate of calcein release was dependent on the concentration of RTA added, but for each RTA concentration the total released calcein could be extrapolated to 100% release. In contrast, addition of ricin holotoxin to calcein-loaded vesicles did not cause calcein release even after prolonged incubation (Figure 8). Similarly, trichosanthin, momordin, and saporin all failed to release calcein from POPG vesicles (Figure 8), consistent with their lack of change in intrinsic protein fluorescence on incubation with POPG vesicles.

RTA Sediments with POPG Vesicles. If RTA binds to POPG vesicles, then it would be expected that bound and unbound protein could be separated by centrifugation. Bound protein should pellet with the vesicles whereas free protein should remain in solution. Figure 9 shows that RTA pellets in the presence of POPG vesicles but remains in solution in the absence of vesicles, or in the presence of DOPC vesicles. In contrast, ricin holotoxin did not pellet with POPG vesicles. Similarly, type I RIPs remained in solution in the presence of POPG, again suggesting that they did not bind to the vesicles.

DISCUSSION

Ricin and a number of other A−B toxins undergo retrograde transport to the ER following cell entry by receptor-mediated endocytosis (*6*−*9*). Subsequent retrotranslocation into the cytosol is mediated by the Sec61 translocon and involves subversion of the ERAD pathway (*7*, *8*). The mechanism by which this class of toxin reaches the ER is slowly being elucidated. However, the events that take place in the ER to facilitate retrotranslocation to the cytosol are poorly understood. It is thought that chain separation is mediated by protein disulfide isomerase (PDI) and that the

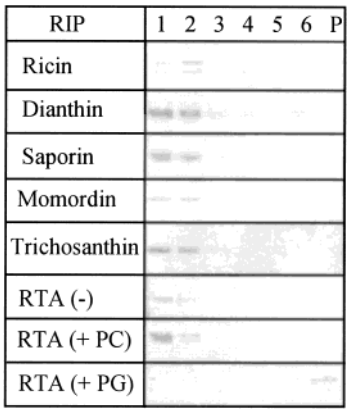

FIGURE 9: Separation of free and lipid-bound RIPs by ultracentrifugation. Mixtures of POPG (200 μM) and RIP (0.1 mg/mL) were incubated at 20 °C for 1 h and then layered onto a 3 mL 0.25 M sucrose pad. Following centrifugation at 100 000 rpm for 1 h, 0.5 mL fractions were removed from the top (lanes 1−6). Pellets were resuspended in 0.5 mL of 0.1% (w/v) SDS (lane P). Fractions were analyzed by SDS PAGE. (−) No addition, (PC) 200 μM DOPC, (PG) 200 μM POPG.

released A-chain can subsequently be recognized as an ERAD substrate. Although some native proteins are regulated by ERAD-mediated degradation (*29*), the majority of known ERAD substrates are misfolded or unassembled protein subunits (*10*−*12*).

Site-directed mutagenesis of both ricin A-chain and SLT A-chain has implicated a hydrophobic stretch of amino acids toward the C-terminal end of these catalytic chains in cytotoxicity (*16*, *18*). A plausible explanation of the observed decrease in cytotoxicity on disruption of this hydrophobic patch, a region that only becomes solvent-exposed on separation of the A- and B-chains, is that this region is required to interact with the ER membrane. Although it has not been demonstrated that membrane interaction is a prerequisite for recognition as an ERAD substrate or for retrotranslocation into the cytosol, such an interaction is an attractive potential mechanism. Partial unfolding induced by interaction of proteins with membrane surfaces has been described previously (*30*−*33*). Thus, membrane-induced partial unfolding of RTA might facilitate recognition as an ERAD substrate. An intact ricin heterodimer is essential for efficient routing to the ER (*2*). Therefore, the region of RTA proposed to interact with membranes only becomes solvent-exposed following chain separation in the ER, thereby targeting RTA to a membrane that possesses the protein-conducting machinery necessary for subsequent translocation into the cytosol.

While several groups have described the interaction of ricin and its component subunits with lipid vesicles, no clear consensus has been reached (*19*−*23*). In the present study, we have used a variety of neutral and negatively charged phospholipids to look for structural changes in ricin or RTA on interaction with phospholipid vesicles. Ricin holotoxin did not interact significantly with any of the lipid vesicles tested as judged by effects on intrinsic protein fluorescence and far-UV CD spectra (Figures 3). Furthermore, ricin did not pellet with vesicles following ultracentrifugation through a 0.25 M sucrose pad (Figure 9), again suggesting that ricin does not form stable complexes with the vesicles.

Although there were no obvious interactions between RTA and neutral (PC) phospholipids, RTA did interact strongly

with negatively charged (PG) phospholipid vesicles. Interaction with POPG vesicles resulted in major changes in both the intrinsic fluorescence and far-UV CD spectra, suggesting that there were substantial changes in both secondary and tertiary structures of the protein. The dramatic (17 nm) blue shift in the fluorescence λ_{max} suggested that one or more of the tyrosyl residues of RTA moved into a more hydrophobic environment, perhaps the lipid bilayer itself. In contrast to an earlier study (*21*), there was no evidence for penetration of the single tryptophan residue of RTA into the lipid bilayer. The tryptophan fluorescence λ_{max} (λ_{ex} 295 nm) of RTA was red shifted by ~8 nm on binding to POPG vesicles, suggesting that the single tryptophan residue moved to a more hydrophilic environment. This change in environment did not, however, alter the ability of iodide to quench the tryptophan fluorescence.

Interaction of RTA with POPG vesicles appeared to be a multistep process. Initial binding could be prevented by preincubation of the vesicles in NaCl prior to addition of RTA, suggesting that binding was an electrostatic process. In contrast, preformed complexes were stable on addition of NaCl, suggesting that after binding, an additional hydrophobic process, possibly membrane insertion, followed. Manual mixing time course experiments were consistent with this two-step process. The observed changes in fluorescence emission at 300 nm could be fitted to single exponentials. However, it was clear that an initial fast phase had been missed, as the time course curves in the presence of POPG did not extrapolate to the same initial fluorescence as that observed for RTA in the absence of lipid. This suggested that initial binding was a fast event and that the observed fluorescence changes were due to structural changes in the protein on insertion into the vesicles.

In contrast to soluble RTA, vesicle-bound RTA was very sensitive to proteolytic cleavage by trypsin, suggesting that the RTA structure had been significantly perturbed. Similarly, vesicle-bound RTA did not bind adenine, suggesting that binding to the vesicles had disrupted the structure of the active site of RTA. Such changes in the structure of RTA could perhaps facilitate binding of chaperones and thereby recognition as an ERAD substrate.

To demonstrate that the interaction of RTA with POPG was a result of the negative charges on the PG headgroup, vesicles composed of phosphatidic acid (DMPA) were also utilized. Incubation of RTA with DMPA vesicles produced the same 17 nm blue shift in the fluorescence λ_{max} as that seen with POPG, suggesting that a similar complex was formed (data not shown). Although higher vesicle concentrations (>1 mM) were required to produce the maximal spectral changes, the final fluorescence spectrum observed was strikingly similar to that for POPG-bound RTA. Separation of DMPA-bound RTA from free RTA by ultracentrifugation showed that when incubated with 200 μM DMPA ~50% of the RTA was bound to the vesicles (data not shown), whereas essentially all of the RTA was bound to POPG under identical conditions (Figure 9). Thus, it is clear that a negatively charged phospholipid headgroup is required to facilitate RTA binding.

If membrane interactions play a crucial role in the intoxication process of ricin, it would be expected that other type II RIPs should also interact with membranes on separation of their A- and B-chains. Indeed, it has been reported earlier that a hydrophobic patch of residues exposed on release of SLT A-chain is involved in cytotoxicity and introduction of charged residues into this region lowers both cytotoxicity and membrane binding (*16*). Furthermore, we have shown that the A-chains of abrin and ebulin only partition into Triton X-114 following reductive separation of their A- and B-chains (Day, Roberts, and Lord, unpublished results). In contrast, it might be imagined that a membrane interactive region would not be conserved in type I RIPs that are not thought to enter the cytosol by Sec61-mediated translocation from the ER. None of the type I RIPs tested (PAP, trichosanthin, dianthin, momordin, and saporin) interacted with any of the lipid vesicles. Their fluorescence spectra were unchanged, they did not release calcein from within vesicles, and they did not co-sediment with vesicles by centrifugation.

Previous studies have demonstrated interactions between ricin and RTA with a variety of vesicle systems. Most of these studies have utilized vesicles formed by sonication of lipid films to form small vesicles, whereas the vesicles in this study were formed by extrusion, which produces larger vesicles. Large extruded vesicles, with a less curved surface, probably better reflect the situation in vivo. The other study to use extruded vesicles (*34*) showed that dianthin did not release calcein from PG or PC vesicles whereas RTA could release calcein only from PG vesicles, consistent with the results presented in this paper.

BIOLOGICAL IMPLICATIONS

Although the data presented in this paper were obtained for RTA interactions with negatively charged phospholipid vesicles in vitro, it is tempting to speculate on the possible outcome of an RTA/lipid interaction in vivo. We propose that on reaching the ER by retrograde transport, the A- and B-chains of ricin are separated by reduction of the interchain disulfide bond. RTA is then exported from the ER to the cytosol, and the only physiological process known to date to facilitate protein export from the ER to the cytosol is the ERAD pathway. The released A-chain can then interact with the ER membrane, facilitating partial unfolding and recognition as an ERAD substrate. The data presented here are consistent with such a hypothesis. RTA, but not ricin, can bind to negatively charged phospholipid vesicles. Binding and subsequent insertion result in a major conformational change in RTA that sensitizes the protein to proteolytic degradation and abolishes product binding, suggesting that it is at least partially unfolded. This altered conformation may resemble that of a misfolded protein, hence permitting recognition by the ERAD machinery.

Finally, it should be stressed that the data presented here were obtained with artificial membranes containing a negatively charged phospholipid (PG) that is not a significant component of the ER membrane. Although the present system is therefore a model one, the ER membrane does contain negatively charged phosphatidylserine. Whether this, or another ER lipid, can induce a conformational change in RTA under physiological conditions remains to be determined.

REFERENCES

1. Lord, J. M., Roberts, L. M., and Robertus, J. D. (1994) *FASEB J. 8,* 201−208.

2. Newton, D. L., Wales, R., Richardson, P. T., Walbridge, S., Saxena, S. K., Ackerman, E. J., Roberts, L. M., Lord, J. M., and Youle, R. J. (1992) *J. Biol. Chem. 267*, 11917−11922.
3. Tsai, B., Rodighiero, C., Lencer, W. I., and Rapoport, T. A. (2001) *Cell 104*, 937−948.
4. Agapov, I. I., Tonevitsky, A. G., Maluchenko, N. V., Moisenovich, M. M., Bulah, Y. S., and Kirpichnikov, M. P. (1999) *FEBS Lett. 464*, 63−66.
5. Endo, Y., Mitsui, K., Motiguki, M., and Tsurugi, K. (1987) *J. Biol. Chem. 262*, 5908−5912.
6. Rapak, A., Falnes, P. O., and Olsnes, S. (1997) *Proc. Natl. Acad. Sci. U.S.A. 94*, 3783−3788.
7. Wesche, J., Rapak, A., and Olsnes, S. (1999) *J. Biol. Chem. 274*, 34443−34449.
8. Schmitz, A., Herrgen, H., Winkeler, A., and Herzog, V. (2000) *J. Cell Biol. 148*, 1203−1212.
9. Jackson, M. E., Simpson, J. C., Girod, A., Pepperkok, R., Roberts, L. M., and Lord, J. M. (1999*) J. Cell Sci. 112*, 467−475.
10. Pilon, M., Schekman, R., and Römisch, K. (1997) *EMBO J. 16*, 4540−4548.
11. Plemper, R. K., Böhmler, S., Bordallo, J., Sommer, T., and Wolf, D. H. (1997) *Nature 388*, 891−895.
12. Brodsky, J. L., and McCracken, A. A. (1997) *Trends Cell Biol. 7*, 151−156.
13. Kopito, R. R. (1997) *Cell 88*, 427−430.
14. Hazes, B., and Read, R. J. (1997) *Biochemistry 36*, 11051−11054.
15. Deeks, E. D., Cook, J. P., Smith, D. C., Day, P. J., Roberts, L. M., and Lord, J. M. (2002) *Biochemistry* (in press).
16. Suhan, M. L., and Hovde, C. J. (1998) *Infect. Immun. 66*, 5252−5259.
17. Chaddock, J. A., Roberts, L. M., Jungnickel, B., and Lord, J. M. (1995) *Biochem. Biophys. Res. Commun. 217*, 68−73.
18. Simpson, J. C., Lord, J. M., and Roberts, L. M. (1995) *Eur. J. Biochem. 232*, 458−463.
19. Menikh, A., Saleh, M. T., Gariepy, J., and Boggs, J. M. (1997) *Biochemistry 36*, 15865−15872.
20. Utsumi, T., Ide, A., and Funatsu, G. (1989) *FEBS Lett. 242*, 255−258.
21. Picquart, M., Nicolas, E., and Lavialle, F. (1989) *Eur. Biophys. J. 17*, 143−149.
22. Ramalingam, T. S., Das, P. K., and Podder, S. K. (1994) *Biochemistry 33*, 12247−12254.
23. Pohl, P., Antonenko, Y. N., Evtodienko, V. Y., Pohl, E. E., Saparov, S. M., Agapov, I. I., and Tonevitsky, A. G. (1998) *Biochim. Biophys. Acta 1371*, 11−16.
24. Helmy, M. E., Lombard, S., and Pieroni, G. (1999) *Biochem. Biophys. Res. Commun. 258*, 252−255.
25. Lombard, S., Helmy, M. E., and Pieroni, G. (2001) *Biochem. J. 358*, 773−781.
26. Bordier, C. (1981) *J. Biol. Chem. 256*, 1604−1607.
27. Watanabe, K., Honjo, E., Tsukamoto, T., and Funatsu, G. (1992) *FEBS Lett. 304*, 249−251.
28. Day, P. J., Ernst, S. R., Frankel, A. E., Monzingo, A. F., Pascal, J. M., Molina-Svinth, M. C., and Robertus, J. D. (1996) *Biochemistry 35*, 11098−11103.
29. Hampton, R. Y. (1998) *Curr. Opin. Lipidol. 9*, 93−97.
30. Pinhiero, T. J. T., Cheng, H., Seeholzer, S. H., and Roder, H. (2000) *J. Mol. Biol. 303*, 617−626.
31. De Jongh, H. H. J., Ritsema, T., and Killian, A. (1995) *FEBS Lett. 360*, 255−260.
32. Shin, I., Kreimer, D., Silman, I., and Weiner, L. (1997) *Proc. Natl. Acad. Sci. U.S.A. 94*, 2848−2852.
33. Shin, I., Silman, I., Bon, C., and Weiner, L. (1998) *Biochemistry 37*, 4310−4316.
34. Lorenzetti, I., Meneguzzi, A., Fracasso, G., Potrich, C., Costantini, L., Chiesa, E., Legname, G., Menestrina, G., Tridente, G., and Colombatti, M. (2000) *Int. J. Cancer 86*, 582−589.

BI012012I